

PACS numbers: 42.55.Lt; 42.60.Mi
DOI: 10.1070/QE2010v040n09ABEH014358

Effect of the pump rate and loss perturbations on the lasing dynamics of a Fabry – Perot laser

N. Kumar, V.I. Ledenev

Abstract. **Transition from generation of the fundamental mode to generation of the fundamental and first modes is studied numerically under the action of nonstationary asymmetric perturbations of pump rate and loss distributions in the active medium layer. It is shown that emergence of perturbations directly leads to excitation of the first mode with significant amplitude. The regime of two-mode lasing in the presence of perturbations is shown to appear at a pump rate that is smaller than the threshold one for two-mode lasing in the absence of perturbations. It is found that the first-mode amplitude has a maximum at a frequency of intermode beatings of an unfilled Fabry – Perot resonator. It is also determined that emergence of nonstationary asymmetric perturbations leads to an increase in the average intensity of the fundamental mode. Various transition regimes to two-mode lasing are compared in different types and periods of perturbations. The operability of the scheme controlling the mode composition of laser radiation is considered.**

Keywords: *laser, Fabry – Perot resonator, lasing dynamics, numerical simulation, control of mode composition of radiation.*

1. Introduction

Nonstationary perturbations of the laser parameters are one of the ways to influence the laser dynamics. Harmonic modulation of the pump rate or resonator losses is used to enable chaotic generation in a single-mode laser [1]. Nonstationary perturbations of the parameters can result from the processes proceeding in the active medium of a laser, for example, radiation self-action in the medium, shock waves appearing because of a pulsed energy input to the active medium of gas lasers, turbulent pulsations of the gas-flow density [2 – 4]. The numerical model of multimode generation in Fabry – Perot lasers was developed in paper [5]. The authors of paper [6] studied numerically transition from generation of one fundamental mode to generation of the fundamental and first modes in the case of a step-wise increase in the uniform pump rate and showed that there appear nonstationary asymmetric perturbations of the active-medium gain distributions. The presence of such perturbations or their artificial simulation can substantially change the characteristics of transition to multimode lasing. It was assumed in [6] that perturbations of the laser parameters are absent. In this paper we study transition from single-mode lasing to two-mode lasing under the action of nonstationary asymmetric perturbations of the pump rate and loss distributions in the active medium layer. We also study the scheme controlling lasing which makes it possible to determine the mode composition of radiations in the presence of the above-mentioned perturbations.

N. Kumar Indira Gandhi Centre for Atomic Research, Kalpakkam 603102, Tamilnadu, India; e-mail: nkumar@rambler.ru;
V.I. Ledenev Institute on Laser and Information Technologies, Russian Academy of Sciences, Svyatoozerskaya ul. 1, 140700 Shatura, Moscow region, Russia; e-mail: ledenev_ilit@rambler.ru

Received 12 May 2010; revision received 22 July 2010
Kvantovaya Elektronika **40** (9) 789 – 793 (2010)
Translated by I.A. Ulitkin

2. Generation model in the presence of perturbations

We studied transition from single-mode lasing to two-mode lasing by using the numerical model [5, 6] where the active medium represented a thin layer located near a highly reflecting resonator mirror. In the plane geometry in the small-angle approximation of the scalar diffraction theory, the electric field inside the resonator was represented in the form of a sum of counterpropagating plane waves modulated by smooth envelopes:

$$E(x,z,t) = [F(x,z,t)\exp(\mathrm{i}k_0 z) + B(x,z,t)\exp(-\mathrm{i}k_0 z)]\exp(-\mathrm{i}\omega_0 t). \quad (1)$$

Here, ω_0 is the carrier frequency; $k_0 = \omega_0/c$. The z axis is directed along the resonator axis while the x axis – along the highly reflecting mirror (see Fig. 1). The envelope dynamics of forward $[F(x,z,t)]$ and backward $[B(x,z,t)]$ waves was described by the equations

$$2\mathrm{i}k_0\left(\frac{1}{c}\frac{\partial B}{\partial t} - \frac{\partial B}{\partial z}\right) + \frac{\partial^2 B}{\partial x^2} - \mathrm{i}k_0 g B + \mathrm{i}k_0 r_\mathrm{L} B = 0, \quad (2)$$

$$2\mathrm{i}k_0\left(\frac{1}{c}\frac{\partial F}{\partial t} + \frac{\partial F}{\partial z}\right) + \frac{\partial^2 F}{\partial x^2} - \mathrm{i}k_0 g F + \mathrm{i}k_0 r_\mathrm{L} F = 0, \quad (3)$$

where $g(x,0,t)$ is the medium gain; $r_\mathrm{L}(x,0,t)$ is the function describing radiation losses in the medium layer. On the resonator mirrors the waves met the reflection conditions

$$F(x,0,t) = -B(x,0,t)r_1, \quad (4)$$

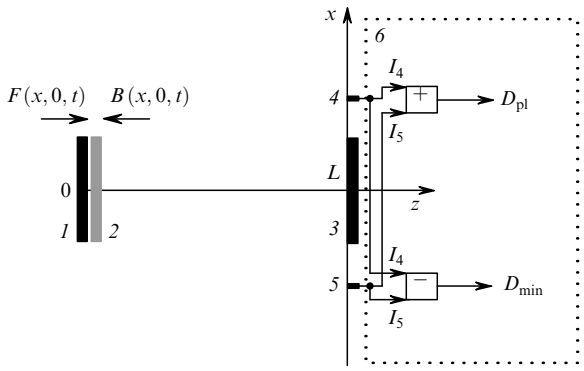

Figure 1. Fabry–Perot laser and the system controlling the mode composition of laser radiation: (*1*) highly reflecting mirror; (*2*) absorbing layer and active medium layer; (*3*) output mirror; (*4, 5*) sensors measuring the field intensity I_4 and I_5; (*6*) processor with circuits transforming the sensor signals; D_{pl} is the total signal from the sensors; D_{min} is the difference signal from the sensors; $F(x,0,t)$, $B(x,0,t)$ are the forward and backward waves in the active medium layer; L is the resonator length.

$$B(x,L,t) = -F(x,L,t)r_2, \tag{5}$$

where r_1 and r_2 are the reflectivities of the highly reflecting and output mirrors.

The equation for the gain in the active medium included the processes of stimulated emission and relaxation with constant time τ:

$$\tau\frac{\partial g}{\partial t} = g_0 - g(1+I),$$
$$I(x,0,t) = |F(x,0,t)|^2 + |B(x,0,t)|^2. \tag{6}$$

Here, $I(x,0,t)$ is the radiation intensity in the active medium layer averaged over the interference beatings of counterpropagating waves and normalised by the saturation intensity [7].

The initial conditions for distributions $F(x,0,0)$, $B(x,L,0)$ and $g(x,0,0)$ corresponded to the established generation of the fundamental mode at a given pump rate $g_0 = g_{0v}$. Perturbation of the pump rate or losses in the active medium layer were introduced at the time instant $t^* = 5$ μs and represented by the periodic function

$$f(x,t) = A_m \sin\left(\frac{2\pi x}{2a}\right)\cos\left[\frac{2\pi(t-t^*)}{T_m}\right], \tag{7}$$

where T_m, A_m are the perturbation period and amplitude of the pump rate or losses in the medium layer. One perturbation wave fitted inside the diameter of the medium layer. The pump rate varied as $g_0(x,t) = g_{0v} + f(x,t)$ and the losses in the medium were described by the function $r_L(x,t) = r_{L0} + f(x,t)$.

Calculations were performed for a Fabry–Perot resonator with the Fresnel number $N_F = 6.25$, plane mirrors of radius $a = 1$ cm, the mirrors being spaced by 150 cm. The radiation wavelength was $\lambda = 10.6$ μm, the reflectivities of highly reflecting and output mirrors were $r_1 = 1$ and $r_2 = 0.8$, and the relaxation time was $\tau = 6.0\times10^{-6}$ s. The parameter $L = 153 \pm 1$ cm and $\lambda = 10.6$ μm corresponded approximately to the parameters of the experimental setup [8, p. 1459]. The laser [9] had a stable resonator with a mirror radius of 5 cm and a constant beam radius of 0.4 cm [8, p. 1461]. At $a = 1$ cm, the radius of the fundamental-mode intensity distributions on a highly reflecting mirror at a 0.5 level was 0.5 cm, which is also close to the beam radius in the active medium in paper [8]. The authors of this paper performed calculations at $\tau = 1.0\times10^{-6}$ s [8, p. 1461]. Test calculations where the relaxation time varied from 3.0×10^{-6} to 1.0×10^{-5} s showed that the behaviour of the time dependences does not experience any noticeable changes. Note also that the value of τ is noncritical in studying the scheme controlling generation.

The system of equations (2)–(6) was solved with the help of the splitting method in terms of physical processes of diffraction and amplification [10]. We used the spectral approach to solve the diffraction part of the problem. The number of network elements was 8192, and the number of elements on the mirror was 512. The system of equations (2)–(6) was time integrated by using an implicit second-order approximation.

In numerical experiments with the pump rate modulation we used the value of g_{0v} below the two-mode lasing threshold by 1.5 % and more, the losses in the medium being absent. The threshold gain g_{th} of the fundamental mode was 1.532×10^{-3} cm^{-1} and for the two-mode lasing it was $g_{th} = 2.023\times10^{-3}$ cm^{-1}.

In numerical experiments with the loss modulation, the pump rate modulation was absent in the medium layer, constant losses in the medium were $r_{L0} = 5.0\times10^{-4}$ cm^{-1}, the loss perturbation amplitude A_L did not exceed 5.0×10^{-4} cm^{-1}. The threshold gain of the fundamental mode in the absence of modulation and in the presence of constant losses in the medium was $g_{th} = 2.027\times10^{-3}$ cm^{-1}. In the case of two-mode lasing, the threshold gain was equal to $g_{th} = 2.514\times10^{-3}$ cm^{-1}.

Excess of the pump rate g_0 over the threshold was found from the ratio $k = g_0/g_{th}$ (at $g_{th} = 1.532\times10^{-3}$ cm^{-1}).

Two sensors measuring the radiation intensity, whose readings were used in the scheme controlling the mode composition of radiation, were placed symmetrically with respect to the resonator axis in the plane $z = L$ in the region $|x| > a$ (Fig. 1). We assumed that the radiation intensity was measured periodically, the period between them being much shorter than the perturbation period T_m. We determined numerically the intensity with the help of the sensors during each round-trip transit of radiation in the resonator.

3. Investigation of transition to two-mode lasing

Transition from single-mode lasing to two-mode lasing was studied by projecting the intensity distributions and the gain on the first two Hermite–Gaussian polynomials $\psi_{0,1}(x)$ in expressions

$$I_i(t) = \int_{-a}^{a} I(x,0,t)\psi_i(x)\mathrm{d}x \Big/ \int_{-a}^{a}\psi_i(x)\psi_i(x)\mathrm{d}x,$$
$$g_i(t) = \int_{-a}^{a} g(x,0,t)\psi_i(x)\mathrm{d}x \Big/ \int_{-a}^{a}\psi_i(x)\psi_i(x)\mathrm{d}x, \tag{8}$$

where $i = 0$, 1 and the parameter g is normalised to the double length of the resonator. The dimensional distribution projections on $\psi_0(x)$ (amplitudes of the fundamental modes) yield information on the dynamics of symmetric

parts of the distributions, while the projections on $\psi_1(x)$ (amplitudes of the first modes) – on the dynamics of the asymmetric parts of the distributions, which is related to transition to two-mode lasing and beatings.

The investigations allowed us to find some (significant for practice) peculiarities of transition from single-mode lasing to two-mode lasing. First, transitions under the action of perturbations (7) took place at pump rates below the two-mode lasing threshold in the case of the uniform pump rate. Second, the appearance of the pump rate perturbations or losses in the active medium layer (7) evokes a response in the dynamics of I_1 and g_1 with a delay, significantly smaller than the perturbation period (Fig. 2). In this case, oscillations of I_1 and g_1 turned shifted in-phase by $\pi/2$ (as in paper [6]) and already during the first period had substantial amplitudes (Fig. 2). Third, the time required for establishing oscillations I_1 after their emergence was shorted than in the case of a step-wise increase in the uniform pump rate [6]. As for the perturbations of the spatial pump-rate distribution, the establishment time decreased on average by 80 % and was minimal during the perturbation period equal to the period of the fundamental- and first-mode beatings in an unfilled resonator (Fig. 3a). Perturbations of the spatial loss distribution in the medium layer lead to establishment of oscillations I_1 with more significant changes in the amplitude and less pronounced dependence of the establishment time of the perturbation period (Fig. 3b). In perturbations with the periods T_m in the range $(2.1 - 2.3) \times 10^{-7}$ s, the dynamics of I_1 proved chaotic and we failed to observe transition to harmonic modulations at times ~ 150 μs in the case of loss modulation (Fig. 3c). Note in this connection that the frequencies of the chaotic dynamics are determined in this case by the beating frequency of two transverse modes, i.e., eigenvalues and the round-trip transit time for radiation in the resonator, and are not linked with the relaxation time of the active medium, which is important for practice. However, the investigation was performed using the second-order approximation and the conclusion drawn are only preliminary. Fourth, the calculations showed that two-mode lasing appears under the action of perturbations in the active medium layer (7) at pump rates below the single-mode lasing threshold (for the uniform pump rate) (Fig. 4). In this case the initial conditions for the distributions $F(x,0,0)$, $B(x,L,0)$ and $g(x,0,0)$ had maximal values at the noise level ($\sim 10^{-14}$) and transition processes continued within hundreds of microseconds.

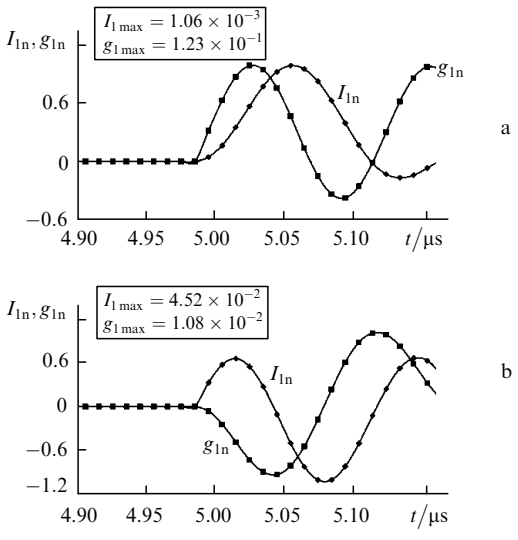

Figure 2. Dynamics of normalised intensities $I_{1n}(t)$ and the mode gain $g_{1n}(t)$ at the beginning of two-mode lasing development $\{I_{1n}(t) = I_1(t)/I_{1\max}$ and $g_{1n}(t) = g_1(t)/g_{1\max}$, where $I_{1\max}$ and $g_{1\max}$ are the maximal values of $|I_1(t)|$ and $|g_1(t)|$ on the interval [0, 5.16 μs]$\}$ in the case of modulation of the pump rate distribution at $g_{0v} = 1.992 \times 10^{-3}$ cm^{-1}, $T_m = 1.3 \times 10^{-7}$ s, $A_m = 0.996 \times 10^{-3}$ cm^{-1} (a) and modulation of loss distributions at $g_{0v} = 2.387 \times 10^{-3}$ cm^{-1}, $T_m = 1.3 \times 10^{-7}$ s, $A_m = 5.0 \times 10^{-4}$ cm^{-1} (b).

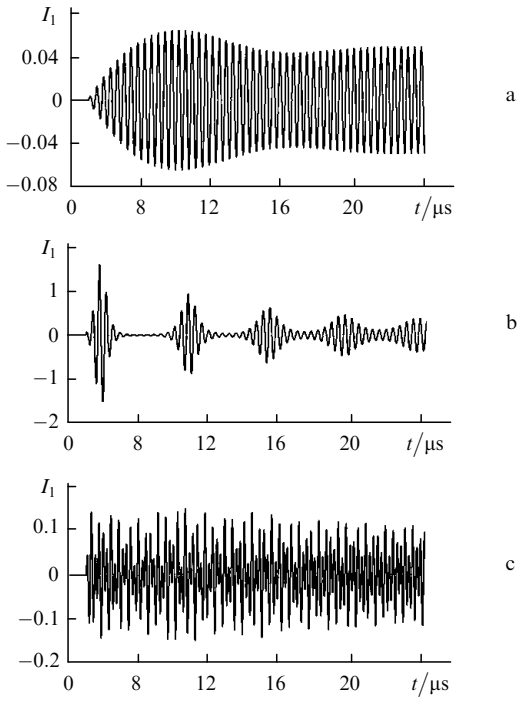

Figure 3. Dynamics of $I_1(t)$ within the first 20 μs after switching on modulation of the pump rate distribution at $g_{0v} = 1.992 \times 10^{-3}$ cm^{-1}, $A_m = 0.996 \times 10^{-3}$ cm^{-1}, $T_m = 3.8 \times 10^{-7}$ s (a) and after switching on modulation of loss distributions in the medium layer at $g_{0v} = 2.387 \times 10^{-3}$ cm^{-1}, $A_m = 5.0 \times 10^{-4}$ cm^{-1} (b, c) [$T_m = 3.8 \times 10^{-7}$ s (b) and 2.2×10^{-7} s (c)].

The oscillation period of the intensity projection I_1 coincided with the period of introduced perturbations. The amplitude of the established oscillations of the intensity projection I_1 had a maximum during the perturbation period equal to the period of the fundamental- and first-

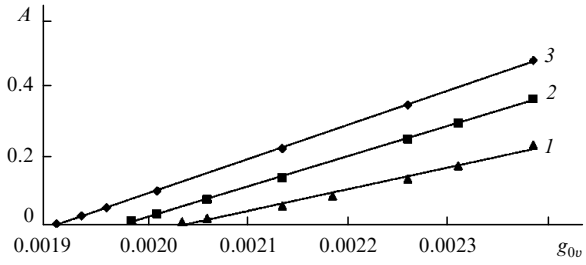

Figure 4. Dependences of the amplitude A of established oscillations $I_1(t)$ on the given pump rate g_{0v} at $A_m = 1.0 \times 10^{-4}$ (*1*), 3.0×10^{-4} (*2*) and 5.0×10^{-4} cm^{-1} (*3*); $T_m = 3.8 \times 10^{-7}$ s.

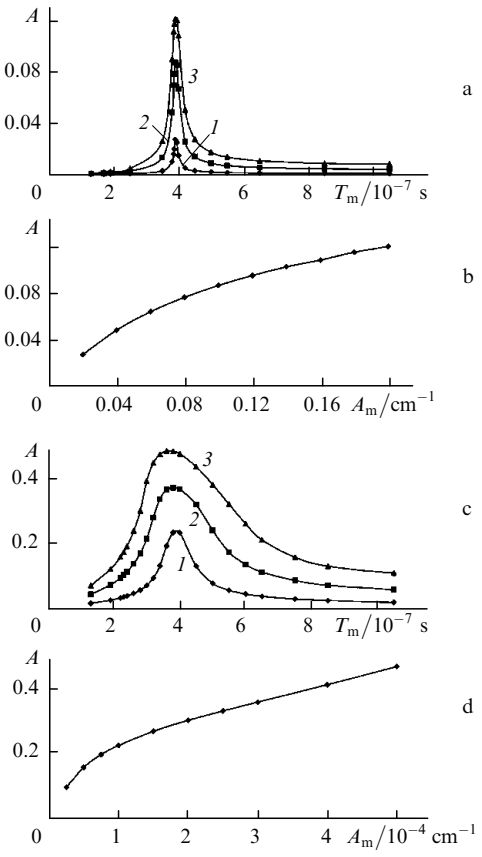

Figure 5. Dependences of the amplitude A of established oscillations $I_1(t)$ on the perturbation period T_m in the case of modulation of the pump rate distribution, $g_{0v} = 1.992 \times 10^{-3}$ cm^{-1}, $T_{empt} = 3.9 \times 10^{-7}$ [$A_m = 0.199\times 10^{-3}$ (*1*), 0.996×10^{-3} (*2*) and 1.992×10^{-3} cm^{-1} (*3*)] (a) on the perturbation amplitude A_m in the case of modulation of the pump rate distribution $g_{0v} = 1.992 \times 10^{-3}$ cm^{-1} and $T_{empt} = 3.9 \times 10^{-7}$ s (b), on the perturbation period in the case of modulation of the loss distribution in the medium layer, $g_{0v} = 2.387 \times 10^{-3}$ cm^{-1}, $T_{empt} = 3.8 \times 10^{-7}$ s [$A_m = 1.0 \times 10^{-4}$ (*1*), 3.0×10^{-4} (*2*) and 5.0×10^{-4} cm^{-1}] (*3*), constant losses in the medium are equal to 5.0×10^{-4} cm^{-1}] (c), and on the perturbation amplitude in the case of modulation of loss distribution in the medium layer, $g_{0v} = 2.387 \times 10^{-3}$ cm^{-1} and $T_{empt} = 3.8\times 10^{-7}$ s.

mode beatings in an unfilled resonator T_{empt} (Figs 5a, c) and increased with increasing the perturbation amplitude (Figs 5b, d).

The appearance of oscillations I_1 and g_1 under the action of nonstationary inhomogeneous perturbations of the pump rate and loss distributions in the medium layer lead to a change in I_0 and g_0 (Fig. 6; only the dependences of I_0 are shown). Especially noticeable were changes in the case of loss modulation in the medium layer. Here, at $t < t^*$, I_0 could increase by an order of magnitude from the level $I_0 = \text{const}$ (first peak in Fig. 6b). During relaxation oscillations of I_0 established and the time-average fundamental-mode intensity increased.

4. Control of the mode composition of radiation

In the previous section we showed that emergence of nonstationary inhomogeneous perturbations of the pump rate or loss distributions leads to the appearance of two-mode lasing. The scheme controlling the mode composition of radiation should indicate the emergence of the first mode

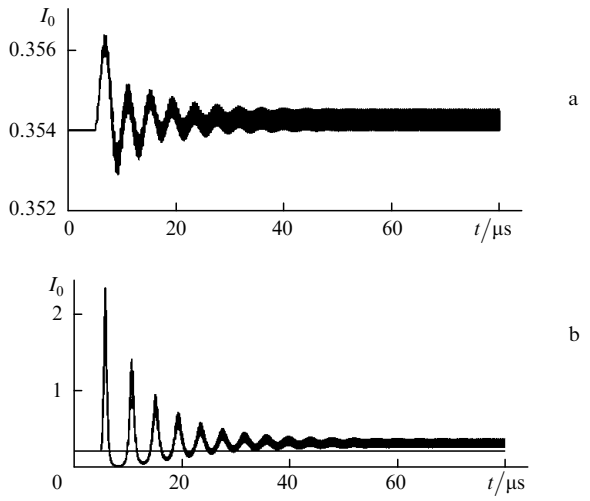

Figure 6. Dynamics of $I_0(t)$ within the first 75 μs after switching on modulation of the pump rate distribution at $g_{0v} = 1.992 \times 10^{-3}$ cm^{-1}, $T_m = 3.8 \times 10^{-7}$ s, $A_m = 0.996 \times 10^{-3}$ cm^{-1} (a) and after switching on modulation of the loss distributions in the medium layer at $g_{0v} = 2.387 \times 10^{-3}$ cm^{-1} [$T_m = 3.8 \times 10^{-7}$ s, $A_m = 5.0 \times 10^{-4}$ cm^{-1} (*1*) and without switching on modulation of the loss distribution (*2*)] (b).

and evaluate the projections $I_{0,1}(t)$ by the sensor signals. As in paper [6] we can determine the emergence of the first mode by the difference signal $D_{min}(t) = |I_4(t) - I_5(t)| \geqslant 0$. More difficult, however, is to lay down rules according to which the scheme controlling the mode composition should assess the dependences $I_{0,1}(t)$. In paper [6], the determination of $I_{0,1}(t)$ was based on calculations of the process of beating establishment at a known excess of the pump rate over the threshold k. Similarly, we can determine it in this case. We assume that the perturbation (7) has the known amplitude A (for example, it is simulated artificially) and the process of beating establishment is calculated. Then, the total $[D_{pl}(t) = I_4(t) + I_5(t)]$ and difference $[D_{min}(t) = |I_4(t) - I_5(t)| \geqslant 0]$ signals can be approximated to $I_0(t)$ and $I_1(t)$ with the help of linear transformations $\alpha D_{pl}(t) + \delta_0$ and $\beta D_{min}(t) + \delta_1$. Operations performed by the processor [6] are supplemented with additions, which should not increase significantly the calculations time, and the values of α, β, δ_0 and δ_1 are extracted from the database. Such an approximation of $I_{0,1}(t)$ was used for different perturbations with various periods and amplitudes. The results are shown in Fig. 7; one can see that $I_0(t) \approx \alpha D_{pl}(t) + \delta_0$ and $I_1(t) \approx \beta D_{min}(t) + \delta_1$ with good accuracy. When the perturbation characteristics are unknown, it is impossible to obtain the coefficients $\alpha, \delta_0, \beta, \delta_1$. Nevertheless, the control scheme can provide us with important qualitative information on the emergence of beatings, on a relative increase in the amplitude, and on the appearance of relaxation fundamental-mode oscillations.

5. Conclusions

Generation in lasers that are used in modern technological processes and are under the action of mechanical vibrations, perturbations in the electric pump circuits, and complicated processes in the active medium can differ significantly from model theories. Numerical investigations performed in this paper have shown that the characteristics such as the thresholds of single-mode and two-mode lasing

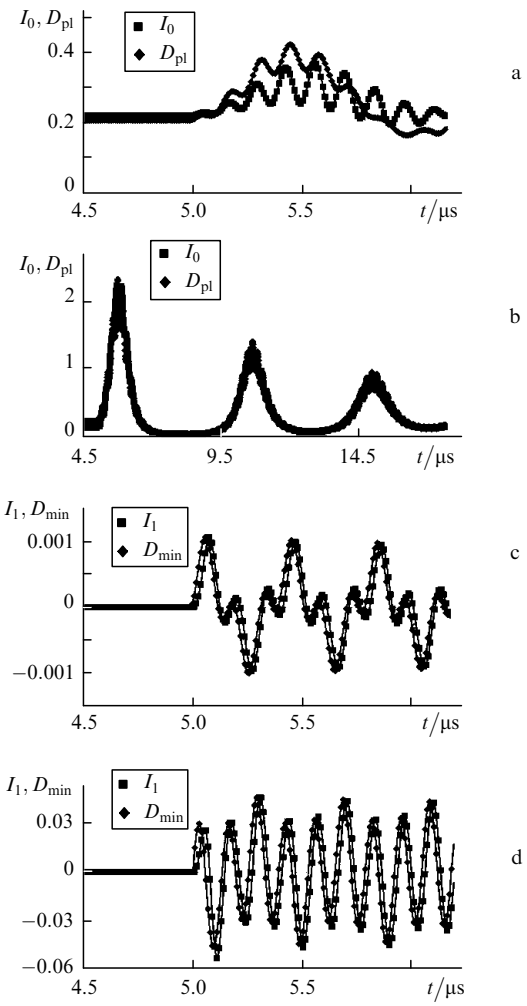

Figure 7. Dependences of $I_0(t)$ and $\alpha D_{pl}(t) + \delta_1$ in the case of modulation of the loss distribution in the medium layer and $g_{0v} = 2.387 \times 10^{-3}$ cm^{-1}, $T_m = 2.6 \times 10^{-7}$ s, $A_m = 5.0 \times 10^{-4}$ cm^{-1}, $\alpha = 5.04$, $\delta_1 = 0.184$ (a) and $g_{0v} = 2.387 \times 10^{-3}$ cm^{-1}, $T_m = 3.8 \times 10^{-7}$ s, $A_m = 5.0 \times 10^{-4}$ cm^{-1}, $\alpha = 2.12$, $\delta_1 = 0$ (b), as well as the dependences of $I_1(t)$ and $\beta D_{min}(t) + \delta_2$ in the case of modulation of the pump rate distribution and $g_{0v} = 1.992 \times 10^{-3}$ cm^{-1}, $T_m = 1.3 \times 10^{-7}$ s, $A_m = 0.996 \times 10^{-3}$ cm^{-1}, $\alpha = -10.1$, $\delta_2 = 0$ (c) and in the case of modulation of the loss distribution in the medium layer and $g_{0v} = 2.387 \times 10^{-3}$ cm^{-1}, $T_m = 1.3 \times 10^{-7}$ s, $A_m = 5.0 \times 10^{-4}$ cm^{-1}, $\alpha = -9.39$, $\delta_2 = 0$ (d).

for unperturbed pump and stationary losses have a limited applicability. We have found the possibility of lasing transition to the chaotic regime in the case of asymmetric spatial modulation of radiation losses in the medium layer according to the harmonic law (7). Investigations of the control scheme with two sensors have shown that its possibilities are sufficient to determine the characteristics of two-mode lasing in the presence of perturbations.

References

1. Khanin Ya. I. *Principles of Laser Dynamics* (Amsterdam, North-Holland: Elsevier, 1995; Moscow: Nauka, 1999).
2. Koval'chuk L.V., Sherstobitov V.E. *Kvantovaya Elektron.*, **4**, 2166 (1977) [*Sov. J. Quantum Electron.*, **7**, 1239 (1977)].
3. Koval'chuk L.V., Sergeev V.V., Sherstobitov V.E. *Kvantovaya Elektron.*, **6**, 1164 (1979) [*Sov. J. Quantum Electron.*, **9**, 687 (1979)].
4. Koval'chuk L.V., Malakhov L.N., Sherstobitov V.E., et al. *Kvantovaya Elektron.*, **10**, 397 (1983) [*Sov. J. Quantum Electron.*, **13**, 221 (1983)].
5. Elkin N.N. *Mat. Model.*, **10** (4), 91 (1998).
6. Kumar N., Ledenev V.I. *Kvantovaya Elektron.*, **40**, 363 (2010) [*Quantum Electron.*, **40**, 363 (2010)].
7. Zvetlo O. *Principles of Lasers* (New York: Plenum Press, 1998; Moscow: Mir, 1990).
8. Coates A.B., Weiss C.O., Green C., et al. *Phys. Rev. A*, **49**, 1452 (1994).
9. Brambilla M., Cattaneo M., Lugiato L.A., et al. *Phys. Rev. A*, **49**, 1427 (1994).
10. Marchuk G.I. *Splitting and Alternating Direction Methods, Handbook of Numerical Analysis*. Ed. by P.G. Ciarlet, J.L. Lions (Amsterdam: North-Holland, 1990) Vol. 1, pp 197 – 462.